Brillouin light scattering study of exchange-coupled Fe/Co magnetic multilayers

2005 J. Phys.: Condens. Matter 17 6483

(http://iopscience.iop.org/0953-8984/17/41/018)

INSTITUTE OF PHYSICS PUBLISHING JOURNAL OF PHYSICS: CONDENSED MATTER

J. Phys.: Condens. Matter **17** (2005) 6483–6494 doi:10.1088/0953-8984/17/41/018

Brillouin light scattering study of exchange-coupled Fe/Co magnetic multilayers

L Giovannini[1], S Tacchi[2], G Gubbiotti[3], G Carlotti[2,4], F Casoli[5] and F Albertini[5]

[1] Dipartimento di Fisica, Università di Ferrara and Istituto Nazionale per la Fisica della Materia, Via Saragat 1, I-44100 Ferrara, Italy
[2] Dipartimento di Fisica, Università di Perugia and Istituto Nazionale per la Fisica della Materia, Via A Pascoli, I-06123 Perugia, Italy
[3] Research Centre SOFT-INFM-CNR, Università di Roma 'La Sapienza' I-00185, Roma, Italy
[4] National Research Centre S3, INFM-CNR, Modena, Italy
[5] IMEM-CNR, Parco Area delle Scienze 37/A, I-43010 Fontanini, Parma, Italy

Received 25 May 2005, in final form 28 July 2005
Published 30 September 2005
Online at stacks.iop.org/JPhysCM/17/6483

Abstract

A combined experimental and theoretical Brillouin light scattering study of thermally excited spin waves in Fe/Co multilayers with three and five magnetic layers in direct contact is presented. A large number of discrete, well-resolved peaks, classified as either surface or bulk standing modes of the stack, appear in the measured spectra. The investigation of their frequency dependence on the magnetic field intensity and incidence angle of light allowed us to determine the complete set of magnetic parameters of the multilayer. The interlayer exchange coupling and perpendicular interface anisotropy are discussed in detail. The profiles of the dynamic magnetization associated with different spin wave modes are calculated and utilized for the calculation of the Brillouin scattering cross section. The result, compared with experimental spectra, allowed the determination of the ratio between the magneto-optic constants of Fe and Co.

Although multilayered structures, composed of alternating magnetic and non-magnetic layers, have been extensively studied in recent years [1], only a few experimental reports on spin waves in multilayers consisting of different ferromagnetic layers in direct contact with each other are available in the literature [2]. Several peculiarities characterize such a system: the absence of a non-magnetic spacer gives rise to a strong interlayer coupling; the surface anisotropies at the interfaces are substantially affected by the direct contact; the coupling between a light probe and the magnetization in the system depends on the relative magneto-optical efficiencies of the different materials.

The theoretical description of the dynamics of the magnetization can be challenging, due to the large number of equations required to describe a system made of many coupled magnetic layers; moreover, if the layers are not thinner than 3–5 nm, it is essential to take into account

the dependence of the magnetization on the coordinate perpendicular to the surface in order to get reliable results. A previous model calculation for an Fe/Ni multilayer, based on the literature bulk values of the magnetic parameters, allowed the study of the dependence of the spin wave frequency on the film thickness and the mode profiles, but without comparison with experimental data [3, 4]. A study of an Ni/Fe bilayer showed that, in the case of ultrathin films, the experimental results can be interpreted in terms of an effective medium, with magnetic properties given by a combination of the magnetic properties of the individual layers [5]. Brillouin light scattering (BLS) from thermally excited spin waves proved to be a valuable experimental technique for studying the magnetic properties of films and multilayers, thanks to the large amount of magnetic information which can be obtained from analysis of BLS spectra [1].

In this paper we present the result of a BLS investigation of spin waves in a thick Cu/Fe/$[Co/Fe]_N$/Cu/Si magnetic multilayer, with $N = 1, 2$, deposited at room temperature by RF sputtering. A detailed study of the spin wave frequency dependence on both the intensity of the external applied magnetic field and the incidence angle of light enabled us to achieve a determination of the magnetic parameters of the system, including the interlayer exchange constant contained in the Hoffman boundary conditions [6]. The dependence of the dynamic magnetization on the perpendicular coordinate is fully taken into account, together with intralayer exchange. The measured Brillouin cross section has been compared with the spectra calculated taking into account the complex ratio between the magneto-optic constants of Co and Fe, allowing the determination of this parameter.

In section 1 the experimental procedure is presented, together with the description and characterization of the samples studied in this work; the theoretical aspects of spin wave propagation in a coupled magnetic multilayer and their interaction with light are discussed in section 2 with some model calculations; the comparison between experimental and theoretical results is shown in section 3. Section 4 is devoted to the discussion of the physical parameters deduced from the analysis of the spectra; finally, in section 5 the Brillouin cross section results are discussed.

1. Sample preparation and experiment

Two multilayers were produced, with three and five magnetic layers in direct contact, according to the following layered structures:

- Sample A: Si/Cu/Fe/Co/Fe/Cu.
- Sample B: Si/Cu/Fe/Co/Fe/Co/Fe/Cu.

All the Fe and Co films are 10 and 20 nm thick, respectively. The multilayers were deposited on oxidized (100) Si substrates, using a Cu underlayer and capping layer, both 5 nm thick. During the deposition, the power supplied to the Co and Cu targets was kept at 150 W and the Ar pressure was maintained at 1.4×10^{-2} mbar. The base pressure of the system was 3×10^{-8} mbar. Homogeneous thickness for the layers was ensured by oscillating the substrate in front of the targets. Two single Co and Fe films, with thickness of 20 and 10 nm, respectively, were also produced and used as reference samples to determine the magnetic properties of the two magnetic materials. Structural and morphological characterization provides accounts for well-defined layered structure with polycrystalline Co and Fe layers with hcp and bcc phases, respectively. From alternating-gradient field magnetometry (AGFM) measurements of the single Co and Fe films, the saturation magnetization values were estimated to be $M_s(\mathrm{Co}) = 1450 \pm 100$ G and $M_s(\mathrm{Fe}) = 1580 \pm 100$ G, respectively. The hysteresis loops measured for the multilayer samples, with the field applied parallel to the film plane,

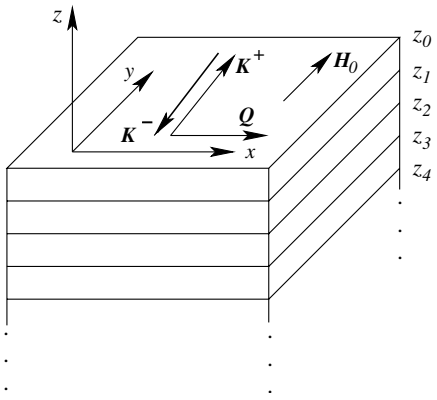

Figure 1. Experimental geometry. The direction of the applied external field ($\boldsymbol{H}_0 \parallel y$) and the magnon wavevector in the anti-Stokes case ($\boldsymbol{Q} \parallel x$) are shown, together with the reference frame. The incident ($\boldsymbol{K}^-$) and scattered ($\boldsymbol{K}^+$) light wavevectors lie in the xz-plane.

revealed a 100% remanence and a coercive field of about 20 Oe. No evidence was found for any appreciable in-plane magnetic anisotropy. For the BLS measurements, about 200 mW of monochromatic P-polarized light, from a single-mode, diode-pumped solid state laser ($\lambda = 532$ nm line), was focused onto the sample surface using a camera objective of numerical aperture 2 and focal length 50 mm [7]. The back-scattered light was analysed by a Sandercock-type (3 + 3)-pass tandem Fabry–Perot interferometer [8]. In the back-scattering geometry, the conservation of momentum in the photon–magnon interaction implies that the spin wave wavevector parallel to the film surface Q is linked to the optical wavelength of light λ and to the angle of incidence θ by the equation $Q = 4\pi \sin\theta/\lambda$. The external dc magnetic field was applied parallel to the surface of the film and perpendicular to the plane of incidence of light. The experimental geometry and the reference frame are shown in figure 1.

2. Theoretical framework

When two magnetic layers are placed in direct contact, a strong ferromagnetic coupling is to be expected. Such coupling does not affect the ground state of each layer, which is dependent on the external field only. However, the calculation of the dynamic magnetization must properly take into account the interlayer coupling in order to reproduce the actual dynamic properties. We extend here the continuum model developed in [9] in order to include the coupling arising from exchange interactions, corresponding to a surface energy density of the form

$$E_{\text{inter}} = -J\frac{\boldsymbol{M}^{(l)}\boldsymbol{M}^{(l+1)}}{M^{(l)}M^{(l+1)}},$$

where $\boldsymbol{M}^{(l)}$ and $\boldsymbol{M}^{(l+1)}$ are the magnetizations of the two layers calculated at the interface, and J is the interlayer coupling constant [6], assumed the same at all interfaces. The magnetization in each layer l is written as a sum of a static and a small dynamic term:

$$\boldsymbol{M}^{(l)}(x,z,t) = \boldsymbol{M}_{\text{s}}^{(l)} + \boldsymbol{m}^{(l)}(x,z,t),$$

so the total magnetic field is

$$\boldsymbol{H}^{(l)}(x,z,t) = \boldsymbol{H}_0 + \boldsymbol{h}^{(l)}(x,z,t),$$

where $\boldsymbol{M}_{\text{s}}^{(l)}$ is the saturation magnetization and $\boldsymbol{H}_0$ is the external field, both lying in the film plane. Dealing with magnetic films several nm thick, the perpendicular dependence of the

dynamic magnetization must be taken into account; therefore, the dynamic magnetization in each film is expanded in partial waves:

$$\boldsymbol{m}^{(l)}(x,z,t) = \mathrm{e}^{\mathrm{i}(Qx-\Omega t)} \sum_{\lambda=1}^{6} a_\lambda^{(l)}(Q,\Omega)\boldsymbol{m}_\lambda^{(l)}(Q,\Omega)\mathrm{e}^{\mathrm{i}q_\lambda^{(l)}z}.$$

Here Ω, the frequency of the magnetic excitation, plays the role of a free parameter, to be determined later. While the parallel component Q of the wavevector is fixed, being determined by the experimental geometry, the perpendicular components $q_\lambda^{(l)}$ must be calculated by imposing the linearized Landau–Lifshitz and Maxwell equations. This procedure also gives the polarization of each partial wave $\boldsymbol{m}_\lambda^{(l)}$. The amplitudes of the partial waves are then obtained by imposing the boundary conditions at each interface, corresponding to the continuity of $h_1^{(l)}$ and of $h_3^{(l)} + 4\pi m_3^{(l)}$. In addition, the total surface torque must vanish. The last condition, written at the interface between two exchange-coupled magnetic layers, differs from the condition written at the interface between magnetic and non-magnetic layers, given in appendix A of [9]. The modified equations are

$$\left[-\frac{2k_{sl}^{\pm}}{M_s^{(l)}}m_3^{(l)} + \frac{2A^{(l)}}{M_s^{(l)}}\frac{\partial m_3^{(l)}}{\partial \boldsymbol{n}} - J\frac{m_3^{(l-1)}}{M_s^{(l-1)}} + J\frac{m_3^{(l)}}{M_s^{(l)}}\right]_{z_\alpha} = 0 \tag{1}$$

$$\left[-\frac{2k_{pl}^{\pm}\sin^2(\Phi_l)}{M_s^{(l)}}m_1^{(l)} - \frac{2A^{(l)}}{M_s^{(l)}}\frac{\partial m_1^{(l)}}{\partial \boldsymbol{n}} + J\frac{m_1^{(l-1)}}{M_s^{(l-1)}} - J\frac{m_1^{(l)}}{M_s^{(l)}}\right]_{z_\alpha} = 0. \tag{2}$$

For each magnetic layer l there are two couples of such equations, calculated at the upper surface ($\alpha = l-1$) and at the lower one ($\alpha = l$); $\boldsymbol{n}$ is the surface normal, pointing inwards. As a consequence, there are two coupled equations at each interface, linking the magnetizations $\boldsymbol{m}^{(l)}$ and $\boldsymbol{m}^{(l-1)}$ calculated at the interface. Here k_{sl}^{+} and k_{sl}^{-} are the surface perpendicular anisotropy constants at the upper and lower surfaces of layer l, respectively, with their sign chosen so that a positive sign indicates an easy axis perpendicular to the film; $k_{pl}^{\pm}$ are the in-plane surface anisotropy constants, set to zero in the application presented in this paper; $A^{(l)}$ is the intralayer exchange constant of the layer l. The meaning of other symbols is given in [9]. These equations, together with the continuity conditions for the fields, give rise to a homogeneous linear system. The frequencies Ω that make the corresponding determinant vanish give the spin resonances; the corresponding partial wave amplitudes $a_\lambda^{(l)}$ are then calculated, allowing the determination of the dynamic magnetization field for each spin mode of the structure.

We focus our attention on the interlayer coupling, that originates from two sources: the exchange interaction between the two different atomic layers at the interface and the dipolar coupling. The effect of the dipolar coupling on the spin wave frequency can be appreciated with a model calculation performed on a multilayer simulating sample A described above. In particular, we imagine obtaining the multilayered structure by sticking together alternating Fe and Co magnetic layers, initially very far apart from each other. The spin wave frequencies of the modes of the structure are shown in figure 2 as a function of the separation distance d between the magnetic layers. For large d the layers are uncoupled, and the modes are those expected for independent layers: the surface mode, also named the Damon–Eshbach (DE) mode [10], which is of dipolar type, and bulk modes, also named perpendicular standing spin waves (PSSW), which are of exchange character, and whose dynamic magnetization amplitude oscillates with z, showing one or more nodes along the perpendicular axis (the number of nodes can be used to label the PSSW). In the present case, for large d, the DE modes of iron and cobalt are at 16.7 (EM1 and EM2) and 22.3 GHz (S) respectively, with the DE modes of the two iron layers almost degenerate. When d decreases, the degeneracy is removed due to the large dipolar fields typical of DE modes. The coupling operates also with respect to the cobalt

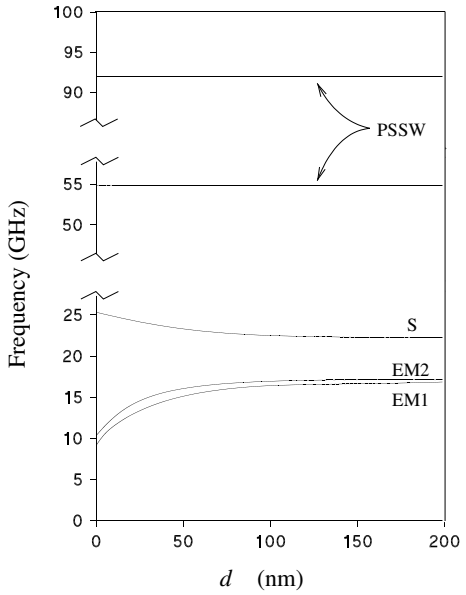

Figure 2. Frequency dependence of the lowest frequency modes of a magnetic trilayer on the interlayer separation d. The constituent layers are Fe (10 nm)/Co (20 nm)/Fe (10 nm), separated by a distance d from each other; the parallel wavevector is $Q = 1.67 \times 10^5$ cm^{-1} and the external field $H_0 = 500$ Oe. The magnetic parameters used in this calculation are shown in table 1.

DE mode, whose dispersion curve is driven toward higher frequencies. In contrast, the first PSSW of cobalt and iron films, at 54.9 and 92.0 GHz respectively, are almost unaffected by the dipolar coupling. In particular, the PSSW modes of the two iron layers remain degenerate, the two layers being separated by (at least) 200 nm of cobalt. In the limit $d \to 0$ this ideal multilayer becomes the appropriate model for representing sample A, except for the interlayer exchange, not included in the calculation of figure 2.

The effect of interlayer exchange J on the frequency of the modes is shown in figure 3. The frequencies of the modes are strongly affected by the coupling, giving rise also to a mode mixing at $J \approx 3$ erg cm^{-2}. The spectrum of a multilayer made of n coupled magnetic layers is thus characterized by a band of n modes originating from the DE mode (low frequency) and higher order PSSW modes. Note also that the curves tend to saturate for large J, a situation corresponding to almost complete alignment of the magnetizations on the two sides of the interfaces. Hillebrands [3, 4] showed the dependence of the spin wave frequencies on the film thickness and interlayer coupling constant (named A_{12} in his papers; $A_{12} = J/2$) for a multilayer Fe/Ni/Fe/Ni/Fe made of layers of equal thickness, 10 nm; however, the different magnetic properties of Co and Ni and the different thicknesses prevent a full comparison with our system. In particular, in our system, the frequency of the first PSSW of the uncoupled Co (20 nm) film is quite low, 54.5 GHz, while that of an Fe (10 nm) film is 92 GHz; instead, for the system studied by Hillebrands, the first PSSW frequency of Ni (10 nm) is just above that of Fe (10 nm). As a consequence, despite the dependence of these frequencies on J (A_{12}) being similar, we did not find the same grouping of modes.

In figure 4 we show the profiles of the dynamic magnetization $\boldsymbol{m}$ calculated for the three lowest frequency modes discussed above, as a function of depth. They have two components, both of which are perpendicular to the applied field. The curves appear as broken lines because

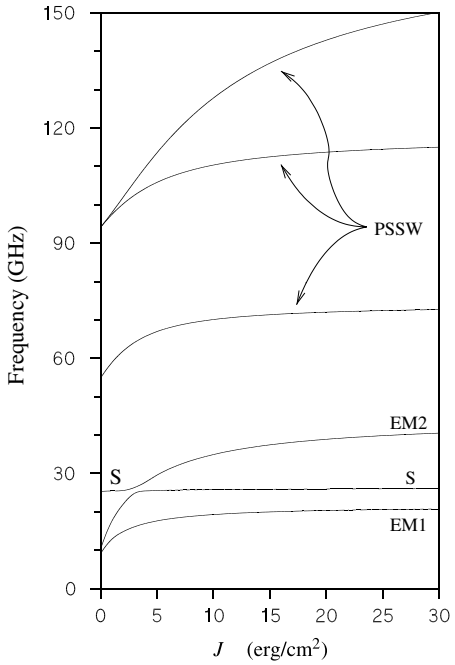

Figure 3. Frequency dependence of the lowest frequency modes of a magnetic trilayer on the interlayer exchange coupling J. The constituent layers are Fe (10 nm)/Co (20 nm)/Fe (10 nm) ($d = 0$); the parallel wavevector is $Q = 1.67 \times 10^5$ cm^{-1} and the external field $H_0 = 500$ Oe. The magnetic parameters used in this calculation are shown in table 1.

the electromagnetic boundary conditions do not require continuity of the magnetization at the interfaces. However, due to the strong interlayer coupling, the discontinuity is relatively small. Note that, despite the three modes of figure 4 deriving from the surface modes of the single layers, the dynamic magnetization in each layer is no longer almost uniform, because of the strong interlayer coupling which deeply modifies the profiles from those of uncoupled single layers. The general behaviour of the profiles allows one to assign the modes of figures 4(a) and (c) to the first and second exchange modes of the structure (EM1 and EM2), showing one and two nodes, respectively. The mode in figure 4(b), having no node, is the surface mode of the structure (S). Its profile resembles that of the usual surface mode of a single magnetic layer (DE mode), which exhibits a dynamic magnetization that slowly decays with depth.

For the Brillouin cross section calculation we adopt a Green's function approach [9], consisting in the solution of the light propagation equation in each layer with a dielectric tensor perturbed by the spin wave. Neglecting second-order effects, the relevant components of the dielectric tensor fluctuations are

$$\delta\epsilon_{21}(x, z) = -K_f m_3(x, z) \tag{3}$$

$$\delta\epsilon_{23}(x, z) = K_f m_1(x, z). \tag{4}$$

The magneto-optic coupling constant K_f is complex and depends on the material f. The scattered light amplitude is a sum of the contributions of the n magnetic layers, properly weighted for taking into account light attenuation and phase shift; therefore the final light intensity depends on the two complex magneto-optic constants K_{Co} and K_{Fe}. The contributions of the two materials are comparable in our samples, because the first magnetic layer (Fe, 100 nm) is thin enough to allow the light scattered by the second layer (Co, 200 nm) to come

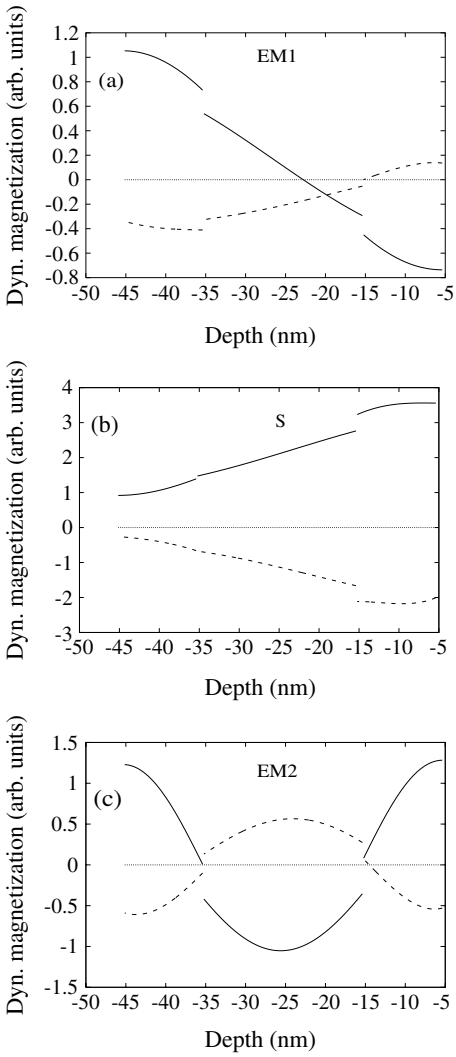

Figure 4. Dynamic magnetization profiles of the modes at 20.23 GHz (a), 25.04 GHz (b) and 38.35 GHz (c) as a function of depth for sample A; the real part of the z component (perpendicular to the surface) and the imaginary part of the x component (in the plane) are shown with solid and dashed lines, respectively. The magnetic parameters used in this calculation are the same as in figure 3, with $J = 17.9$ erg cm^{-2}. The free surface of the sample is located at $z = 0$ (Cu); the surface of the first magnetic layer is at $z = -5.3$ nm.

out without suffering excessive attenuation. This allows the determination of the magneto-optic properties of the structure; in particular, the cross section being equal to the square modulus of the light amplitude and measured apart from a multiplicative constant, the ratio $K_{\mathrm{Co}}/K_{\mathrm{Fe}}$ can be determined.

3. Results

A representative BLS spectrum taken at room temperature for each sample is presented in figure 5. Several well-resolved peaks are present which are identified as the dipolar surface

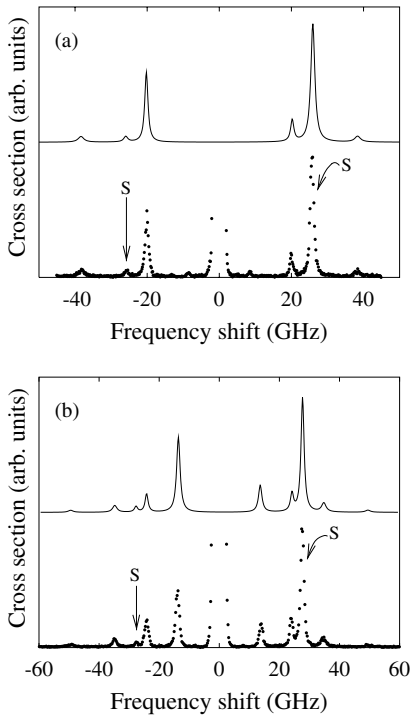

Figure 5. BLS spectra taken from samples A (a) and B (b) with an incidence angle $\theta = 45°$ and an applied field $H_0 = 500$ Oe. Dots: experimental points; lines: calculated cross section (fit). The tiny peaks at ± 8 GHz are not related to magnetic excitations, corresponding instead to ghosts of a surface phonon, visible in the experimental spectra because of the finite extinction ratio of the analyser used in the experiment.

mode (S) and exchange modes (EM), decreasing in intensity for increasing frequency. The marked asymmetry in the intensity of the surface mode is due to the fact that it is a non-reciprocal mode and is localized at the outermost surfaces of the multilayer stack.

Systematic BLS measurements, taken for different values of the applied field (0–4000 Oe) and incidence angle (5°–70°), allowed us to obtain the dispersion curves of the spin modes for the two samples. In figure 6 the experimental frequencies are plotted as a function of the parallel wavevector Q. It can be seen that all the bulk modes (full points) are dispersionless, as expected, while the frequency of the surface modes of the structures (open circles) increases as a function of the incidence angle and crosses that of some bulk modes. In figure 7 the frequency dependence on the external field intensity is shown. These data form the basis of the analysis performed in the following section, together with the results obtained from single Co and Fe films, where the frequency dispersion has been measured versus the applied field and incidence angle (not shown here). In the Co single layer the DE and the first bulk mode have been detected, while in Fe we have only measured the DE mode, because the lowest bulk modes, expected round 100 GHz, fall outside the experimental spectral range.

4. Analysis of the data

We performed a best fit of the calculated frequencies versus the experimental data, in order to find the values of the relevant magnetic parameters of the materials. For this purpose, we

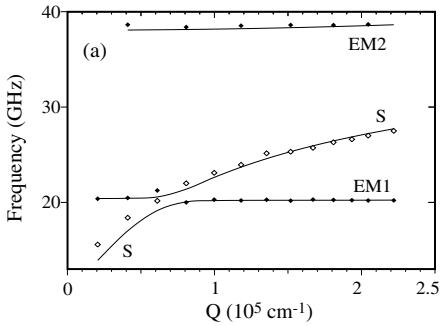

Figure 6. Frequencies of the spin modes of the sample A (a) and B (b) as a function of the parallel wavevector Q. The external field is $H_0 = 500$ Oe. Dots: experimental points; lines: calculated curves (fit).

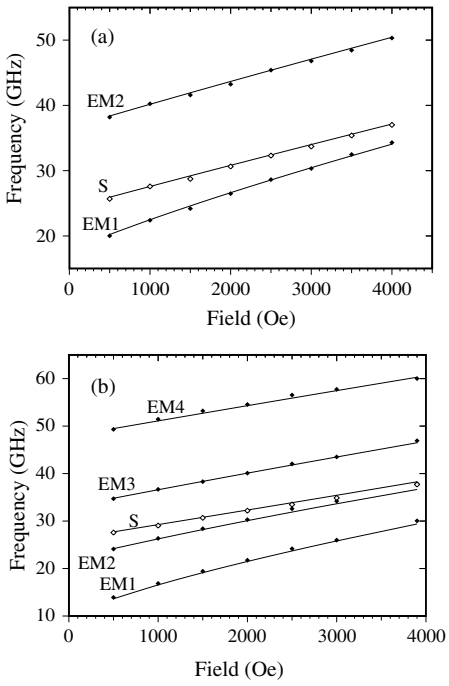

Figure 7. Frequencies of the spin modes of the two samples A (a) and B (b) as a function of the applied field. The incidence angle is 45°, $Q = 1.67 \times 10^5$ cm^{-1}. Dots: experimental points; lines: calculated curves (fit).

exploited the Levenberg–Marquardt numerical method [11], based on the minimization of χ^2:

$$\chi^2 = \sum_{i=1}^{N} \left(\frac{\Omega_{\mathrm{exp}\,i} - \Omega_{\mathrm{th}\,i}}{\sigma} \right)^2,$$

where $\Omega_{\mathrm{exp}\,i}$ are the experimental frequencies, $\Omega_{\mathrm{th}\,i}$ the theoretical ones (depending on the magnetic parameters to be determined) and σ is their standard deviation. The theoretical frequencies are calculated with the model described in section 2, taking fully into account the dependence of the dynamic magnetization on the perpendicular coordinate. We treated separately the two sets of data obtained from samples A and B. In addition, in order to improve the ability to disentangle the parameters of Co and Fe, which contribute together to form the properties of the multilayers, we added to each data set the frequencies found for the spin modes of Co and Fe single films. Using the saturation magnetizations found by alternating gradient field magnetometry, we determined the other parameters for each data set, that is, the magnetic properties of the two ferromagnetic materials (spectroscopic splitting factor g and intralayer exchange constant A) and the interlayer properties, i.e. the out-of-plane interface anisotropy k_s and the bilinear exchange coupling coefficient J. The results are shown in table 1.

The continuous curves in both figures 6 and 7 are calculated with the fitted values of the magnetic parameters, and show a very good agreement with the experimental results. The goodness of the fit can also be represented by the values of χ^2 which are, for the two data sets, 185 and 187; they should be compared with the respective degrees of freedom: 83 and 127. A standard deviation $\sigma = 0.3$ GHz has been assumed, corresponding to the estimated

Table 1. Values of the magnetic parameters of Co and Fe, interface anisotropy and interlayer coupling constant obtained from the fit of the experimental data with the theoretical model, together with the calculated confidence limits for a standard confidence level of 68.3% [11].

Data set	g Co	A Co (10^{-6} erg cm^{-1})	g Fe	A Fe (10^{-6} erg cm^{-1})	$k_{s\ Fe/Co}+k_{s\ Co/Fe}$ (erg cm^{-2})	J (erg cm^{-2})
1 (Sample A)	2.13 ± 0.06	3.05 ± 0.02	1.97 ± 0.08	2.0 ± 0.8	0.47 ± 0.37	17.9 ± 14
2 (Sample B)	2.08 ± 0.07	3.02 ± 0.02	1.99 ± 0.08	2.2 ± 0.2	0.31 ± 0.75	29.5 ± 6.9

experimental error on the measured frequencies; the degrees of freedom are obtained as the difference between the number of experimental data available for the sample (including single-layer data) and the number of fitted parameters.

The two data sets show very close values for the gyromagnetic ratio and exchange constant of both Fe and Co, with small errors; the values obtained are slightly lower but compatible, within the experimental error, with the values reported in the previous BLS literature [12–14]. As regards the surface anisotropies at the interface Co/Fe, $k_{s\ Fe/Co}$ and $k_{s\ Co/Fe}$, an independent fitting of these two parameters is impossible. It is clearly seen from equation (1) that, for $J \to \infty$, the perpendicular anisotropy is cut off, the pinning being completely dominated by the exchange interaction with the bulk. For finite values of J instead, a dependence on the perpendicular anisotropy is retained; in spite of that, if J is large, the magnetizations on either side of the interface tend to coincide, and the two anisotropy constants $k_{s\ Fe/Co}$ and $k_{s\ Co/Fe}$ give rise to the same physical effect. Therefore, in a multilayer made of strongly coupled magnetic layers, only an effective interface anisotropy

$$k_{s\ Fe/Co} + k_{s\ Co/Fe},$$

can be estimated, at most. Our results (table 1) show that, in the present case, the value of the interface anisotropy cannot be determined exactly.

As regards the interlayer coupling J, we actually found very high values with respect to those commonly found in the presence of a non-magnetic interlayer [15, 16]. The large error affecting J is due to the saturation effect discussed in relation to figure 3, which makes the magnon frequencies insensitive to the precise value of J; in addition, in this case the symmetric error bar characteristic of a fit is not fully appropriate. We can reasonably conclude that $J > 8$ and 25 erg cm^{-2}, for samples A and B, respectively. Within our macroscopic approach, no comparison can be made between the interlayer exchange coupling constant, related to the discontinuity of the magnetization $\boldsymbol{M}(x, z, t)$ at an interface $z = z_n$, and the intralayer exchange constant, related to the continuous variation of the magnetization within a given layer $\boldsymbol{\nabla M}$.

5. Brillouin cross section

The experimental spectra, with their well-resolved peaks, allowed a quantitative comparison with the calculated BLS cross section. Figure 5 shows a BLS spectrum measured for each sample, together with the calculated cross section. We notice that the agreement between the calculated and measured Brillouin light scattering spectra is very good. For the calculation we used the following values of the dielectric constants [17–19]: $\epsilon_{Fe} = 0.118 + 17.3i$, $\epsilon_{Co} = -10.4 + 15.66i$, $\epsilon_{Cu} = -5.5 + 5.8i$ and $\epsilon_{Si} = 17.3 + 0.43i$; the ratio between the magneto-optic constants K_{Co}/K_{Fe} acts as a fit parameter.

As described in section 2, any magnetic layer contributes to the Brillouin cross section with a complex amplitude; the modulus and phase correspond to the intensity and phase of

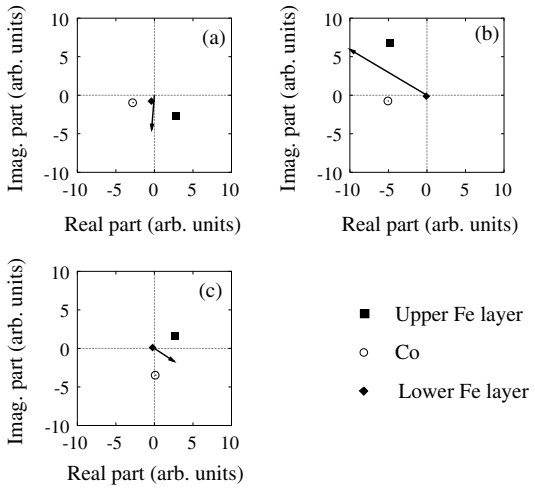

Figure 8. Amplitudes of the anti-Stokes Brillouin cross section due to the three magnetic layers of sample A, for an incidence angle $\theta = 45°$ and an applied field $H_0 = 500$ Oe; the arrows represent the sums of the three complex contributions. Panels (a), (b) and (c) refer to the peaks at 20, 26 and 38 GHz, respectively. The ratio K_{Co}/K_{Fe} is fixed at the best fit value $1.48 + 0.85$i.

the light scattered by the given layer, taking into account the attenuation and phase shift of the incident and scattered light. The complex amplitudes are proportional to the magneto-optic coupling constants of the corresponding material. The complex contribution to the Brillouin cross section of the three magnetic layers of sample A is shown in figure 8 for the three anti-Stokes peaks. The sum of the three complex amplitudes is also shown; its square modulus gives the total cross section. It can be seen that the contribution of the deeper Fe layer is always very small, due to the light absorption. The total cross section is mainly due to the competition of the contributions of the first two layers (Fe and Co). In particular, they can sum to a large contribution, as in figure 8(b), or interfere almost destructively, as in figure 8(c). Such effects, and the ability to theoretically reproduce them, are essential for determining the relative scattering intensity of the two materials. Since the distribution in the magnetic layers of the energy associated with the dynamic magnetization depends on the specific mode, as shown in section 2, the ratio K_{Co}/K_{Fe} can be determined by comparing the Brillouin cross sections of different modes. The best fit procedure leads to the following values: $K_{Co}/K_{Fe} = 1.48 + 0.85$i for sample A and $1.13 + 0.90$i for sample B. A previous study of magneto-optic properties of Fe and Co, based on ellipsometric techniques [20], allowed the measurement of the magneto-optic constants for a light wavelength of $\lambda = 630$ nm. From the measurements reported in [20] we work out $K_{Co}/K_{Fe} = 0.85 + 0.72$i; this value is rather close to our results, despite the different light wavelength.

6. Conclusions

We studied the magnetic properties of Fe/Co multilayers with magnetic layers in direct contact. Several modes were observed in the BLS spectra; their behaviour was investigated as a function of both the magnetic field intensity and the incidence angle of light. By using a best fit procedure, the magnetic properties of the samples have been determined, allowing us to reproduce all the experimental data for each sample with a single set of magnetic parameters. We have been able to explain the nature of the spin modes in connection with

their magnetization profile across the multilayer and discuss the role of interlayer exchange coupling and surface anisotropy at the interface between the magnetic materials. The BLS cross section was calculated and compared to the measured spectra, achieving a very good agreement. From this comparison we were also able to estimate the ratio of the complex magneto-optic constants of Fe and Co.

Acknowledgment

Partial support from Ministero Istruzione, Università e Ricerca (PRIN 2003025857 and FIRB RBNE017XSW), is acknowledged.

References

[1] Hillebrands B 2000 *Light Scattering in Solids VII* (*Springer Series in Topics Applied Physics*) ed M Cardona and G Güntherodt (Berlin: Springer)
[2] D'Orazio F, Lucari F, Carlotti G, Gubbiotti G, Carbucicchio M and Ruggiero G 2001 *J. Magn. Magn. Mater.* **226–230** 1767
[3] Hillebrands B 1988 *Phys. Rev.* B **37** R9885
[4] Hillebrands B 1990 *Phys. Rev.* B **41** 530
[5] Heinrich B, Purcell S T, Dutcher J R, Urquhart K B, Cochran J F and Arrott A S 1988 *Phys. Rev.* B **38** 12879
[6] Hoffmann F, Stankoff A and Pascard H 1970 *J. Appl. Phys.* **41** 1022
[7] http://ghost.fisica.unipg.it
[8] Sandercock J R 1982 *Trends in Brillouin Scattering* vol 3 (Berlin: Springer) p 173
[9] Giovannini L, Zivieri R, Gubbiotti G, Carlotti G, Pareti L and Turilli G 2001 *Phys. Rev.* B **63** 104405
[10] Damon R W and Eshbach J R 1961 *J. Phys. Chem. Solids* **19** 308
[11] Press W H, Teukolsky S A, Vetterling W and Flannery B P 1986 *Numerical Recipes* (Cambridge: Cambridge University Press)
[12] Grimsditch M, Fullerton E E and Stamps R L 1997 *Phys. Rev.* B **56** 2617
[13] Bland J A C, Hicken R J, Eley D E P, Gester M, Gray S J, Daboo C and Ives A J R 1995 *J. Magn. Magn. Mater.* **145** 278
[14] Heinrich B, Urquhart K B, Dutcher J R, Purcell S T, Cochran J F and Arrott S 1988 *J. Appl. Phys.* **63** 3863
[15] Grünberg P, Schreiber R, Pang Y, Brodsky M B and Sovers H 1986 *Phys. Rev. Lett.* **57** 2442
[16] Fassbender J, Nortemann F, Stamps R L, Camley R E, Hillebrands B, Güntherodt G and Parkin S S P 1992 *Phys. Rev.* B **46** R5810
[17] Johnson P B and Christy R W 1974 *Phys. Rev.* B **9** 5056
[18] Johnson P B and Christy R W 1972 *Phys. Rev.* B **6** 4370
[19] Aspnes D E and Studna A A 1983 *Phys. Rev.* B **27** 985
[20] Prinz G A, Maisch W G, Lubitz P, Forester D W and Krebs J J 1981 *IEEE Trans. Magn.* **17** 3232